

Quantum efficiency of the $\text{YAl}_3(\text{BO}_3)_4:\text{Nd}$ self-frequency-doubling laser material

This article has been downloaded from IOPscience. Please scroll down to see the full text article.

1998 J. Phys.: Condens. Matter 10 7901

(<http://iopscience.iop.org/0953-8984/10/35/022>)

View [the table of contents for this issue](#), or go to the [journal homepage](#) for more

Download details:

IP Address: 171.66.16.209

The article was downloaded on 14/05/2010 at 16:43

Please note that [terms and conditions apply](#).

Quantum efficiency of the $\text{YAl}_3(\text{BO}_3)_4:\text{Nd}$ self-frequency-doubling laser material

D Jaque, J A Muñoz, F Cussó and J García Solé

Departamento de Física de Materiales C-IV, Universidad Autónoma de Madrid, 28049-Madrid, Spain

Received 27 May 1998

Abstract. In this paper, the quantum efficiency of the $\text{YAl}_3(\text{BO}_3)_4:\text{Nd}$ laser crystal has been measured using a method based on the simultaneous measurement of photoacoustic and photoluminescence signals within a broad wavelength excitation range (700–850 nm). A quantum efficiency $\Phi = 0.26 \pm 0.05$ is determined. This low quantum efficiency is explained in terms of a high multiphonon relaxation rate from the metastable state ${}^4\text{F}_{3/2}$ involving about three effective phonons of energy 1346 cm^{-1} .

Since the first report of continuous wave (cw) green laser radiation in $\text{LiNbO}_3:\text{MgO}:\text{Nd}$ crystals [1] the research in other non-linear host crystals for the Nd^{3+} ions has been strongly supported [2–5]. Nd^{3+} doped non-linear crystals provide the possibility of realizing compact diode-pumped visible lasers, since external doubling crystals are not necessary. Thus visible radiation can be produced by self-frequency-doubling (SFD) the fundamental infrared radiation of the Nd^{3+} ions. Neodymium-doped yttrium aluminium borate ($\text{YAl}_3(\text{BO}_3)_4$), hereafter referred to as YAB:Nd, has emerged as the most efficient SFD laser crystal at 531 nm [6]. In fact, a number of pulsed and cw green lasers based on this crystal have been already demonstrated under a variety of operating schemes [6–10]. In spite of the high efficiency of this material because of its high non-linear coefficient, high threshold damage, good mechanical properties and high segregation coefficient for neodymium ions, thermal effects can strongly affect its performance, causing instabilities in the laser green power and reducing the slope efficiency [11]. However, in spite of its influence on the laser performance, a direct measurement of the quantum efficiency has not been still carried out in this material.

Photoacoustic spectroscopy is a well known experimental technique for determining quantum efficiencies of ions in solids if an additional technique is used for calibration [12–15]. In this paper the quantum efficiency is measured by using a method based on the simultaneous measurement of both photoacoustic and luminescence signals [16].

Single crystals of YAB:Nd (5.6 at.% of Nd in the crystal) were grown by the flux method in the Institute of Structure of Matter (Fuzhou, China). This Nd concentration is the same as used for an optimum SFD laser [17]. Growth details of the crystal boule have been already described [18]. Plate samples, with a thickness of 1 mm to avoid saturation in the photoacoustic signal, were cut and carefully polished for optical and photoacoustic measurements.

Quasi-continuous-wave excitation at different wavelengths was achieved by using an argon-pumped Ti-sapphire laser (Spectra Physics 3900). The laser beam was chopped at a frequency of 300 Hz. Then, the unpolarized luminescence was collected from one face of the sample to the entrance slit of a monochromator (Spex 0.500M) and detected by a cooled photomultiplier (Hamamatsu R636). The photoacoustic signal was simultaneously recorded attaching a piezoelectric transducer (with a 400 kHz bandwidth) to the opposite side of the sample. Both photoluminescence and photoacoustic signals were amplified and finally recorded using a two channel locking amplifier.

The absorption spectrum of YAB:Nd in the region from 700 to 850 nm consists of two structured bands centred at 750 and 810 nm corresponding to transitions from the ground state ${}^4I_{9/2}$ to the excited states ${}^4F_{7/2}$ and ${}^4F_{5/2}$ respectively [18]. After pumping to these states, a fast non-radiative decay to the metastable state ${}^4F_{3/2}$ takes place. When the ion reaches this metastable state (${}^4F_{3/2}$) it has a probability $1 - \Phi$ (Φ being the quantum efficiency) of decaying non-radiatively to the ground state (${}^4I_{9/2}$) and a probability $\beta_i \Phi$ (where β_i are the branching ratios) of radiative decay to one of the states below the metastable state (4I_J manifold). Finally, when the ion is in one of these states, a non-radiative relaxation to the ground state ${}^4I_{9/2}$ takes place. All these processes are summarized in figure 1.

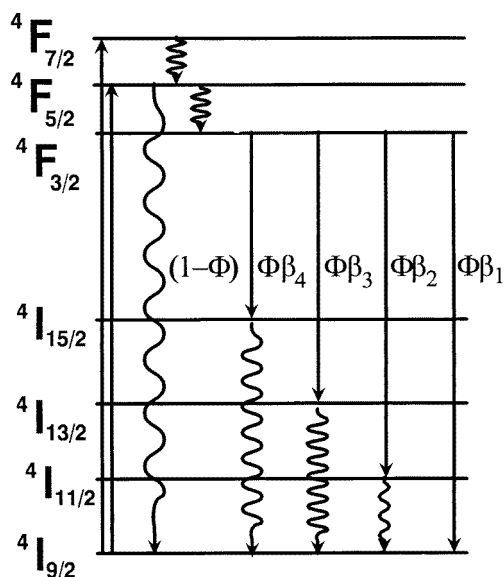


Figure 1. Partial energy level scheme of Nd^{3+} ions in YAB. Arrows represent the different processes (solid—radiative decays, wavy—non-radiative decays) which can take place after the ions reach the excited states 4F_J . The probabilities (Φ and $1 - \Phi$) for these processes are indicated. β_i represent the fluorescence branching ratios.

The photoacoustic signal (PAS), which is proportional to the heat transferred to the sample, can be written as:

$$\text{PAS}(\lambda) = \kappa N(\lambda) \left[\left(\frac{10^7}{\lambda} - E_{4F_{3/2}} \right) + (1 - \Phi) E_{4F_{3/2}} + \left(\sum_i \beta_i E_i \right) \Phi \right] \quad (1)$$

where $N(\lambda)$ is the number of excited ions, κ is a constant which depends on the geometrical

conditions, λ is the excitation wavelength (in nm), β_i the branching ratios from the metastable state ${}^4F_{3/2}$ to the states $i = {}^4I_{9/2}$; ${}^4I_{11/2}$; ${}^4I_{13/2}$ and ${}^4I_{15/2}$ and E_i the energies (in cm^{-1}) of these states i .

In order to calculate the quantum efficiency (Φ), the branching ratios (β_i) must be previously determined. These β_i ratios can be experimentally measured by recording the polarized emission spectra (not shown for the sake of brevity) from the metastable state ${}^4F_{3/2}$ (wavelength range 800–1600 nm). After recording these spectra (using a calibrated germanium detector) values $\beta_i = 0.49, 0.46, 0.05$ and 0 were obtained for the ratios to the ground states ${}^4I_{9/2}$, ${}^4I_{11/2}$, ${}^4I_{13/2}$ and ${}^4I_{15/2}$ respectively. These values are very close to those reported after a Judd–Ofelt analysis of the absorption intensities [18]. Using these β_i ratios a value of $-10\,050 \text{ cm}^{-1}$ for the term $(\sum_i \beta_i E_i) - E_{{}^4F_{3/2}}$ was obtained.

At this point we can estimate the ratio between the integrated PAS in the wavelength ranges involving the excited states ${}^4F_{7/2}$ and ${}^4F_{5/2}$ (728–772 nm and 774–847 nm respectively) so that the constant κ can be removed. This ratio is given by:

$$\frac{\int_{772 \text{ nm}}^{728 \text{ nm}} \text{PAS}(\lambda) d\lambda}{\int_{847 \text{ nm}}^{774 \text{ nm}} \text{PAS}(\lambda) d\lambda} = \frac{\left[\left(\int_{772 \text{ nm}}^{728 \text{ nm}} N(\lambda) \frac{10^7}{\lambda} d\lambda \right) + \left(\Phi(-10\,050) \int_{772 \text{ nm}}^{728 \text{ nm}} N(\lambda) d\lambda \right) \right]}{\left[\left(\int_{847 \text{ nm}}^{774 \text{ nm}} N(\lambda) \frac{10^7}{\lambda} d\lambda \right) + \left(\Phi(-10\,050) \int_{847 \text{ nm}}^{774 \text{ nm}} N(\lambda) d\lambda \right) \right]} \quad (2)$$

Now, in order to evaluate the number of excited ions ($N(\lambda)$) the absorption spectrum can be used. Instead of the absorption spectrum we have taken the excitation spectrum which is proportional to $N(\lambda)$ and has the advantage of giving its actual spectral shape, avoiding the spectral characteristics of the excitation source. In fact, due to the high Nd concentration of our laser crystal $N(\lambda)$ is not proportional to the optical density.

Figure 2 shows the excitation spectrum, i.e. the number of excited ions versus the wavelength, together with the photoacoustic spectrum. From the excitation spectrum in figure 2 is obtained that:

$$\int_{772 \text{ nm}}^{728 \text{ nm}} N(\lambda) d\lambda = \alpha 11.68 \text{ nm}^{-2} \int_{772 \text{ nm}}^{728 \text{ nm}} N(\lambda) \frac{10^7}{\lambda} d\lambda = \alpha 155\,104 \text{ nm}^{-2} \text{ cm}^{-1} \quad (3)$$

$$\int_{847 \text{ nm}}^{774 \text{ nm}} N(\lambda) d\lambda = \alpha 20.26 \text{ nm}^{-2} \int_{847 \text{ nm}}^{774 \text{ nm}} N(\lambda) \frac{10^7}{\lambda} d\lambda = \alpha 250\,701 \text{ nm}^{-2} \text{ cm}^{-1} \quad (4)$$

where α is a constant which takes into account the ratio between the registered intensity and the actual number of excited ions. This constant is not longer necessary as it can be removed in (2).

It should also be noticed in figure 2 that the photoacoustic spectrum does not exactly display the same shape as the excitation spectrum. In particular, the relative PAS corresponding to the ${}^4F_{5/2}$ state is lower than the corresponding relative excitation intensity.

This difference is because of the energy gap between the states ${}^4F_{7/2}$ and ${}^4F_{5/2}$, which is delivered as photoacoustic signal but it does not contribute to the excitation spectrum. From the photoacoustic spectrum it is possible to calculate the integrated PAS ratio (left-hand term in equation (2)):

$$\frac{\int_{772 \text{ nm}}^{728 \text{ nm}} \text{PAS}(\lambda) d\lambda}{\int_{847 \text{ nm}}^{774 \text{ nm}} \text{PAS}(\lambda) d\lambda} = \frac{11.63}{18.39} = 0.63. \quad (5)$$

Substituting the values found in (3), (4) and (5) in equation (2) and solving for Φ , a quantum efficiency $\Phi = 0.26$ is found, within a 20% accuracy.

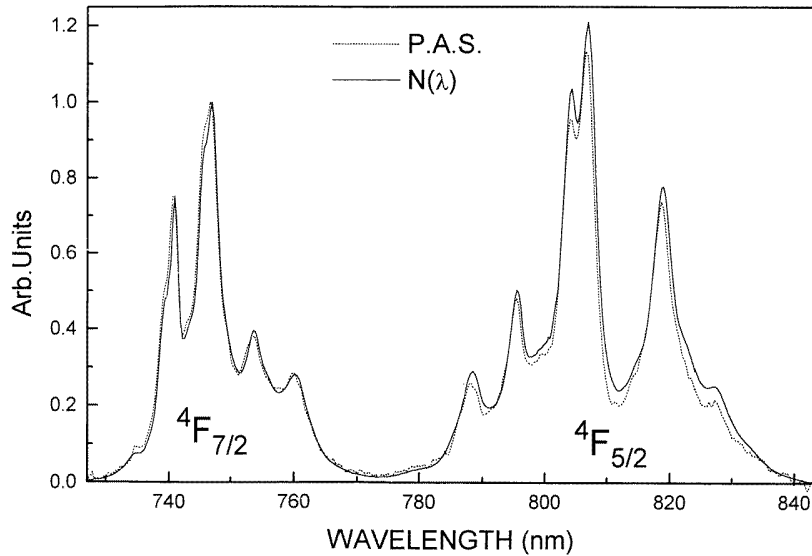


Figure 2. Number of excited ions versus wavelength (excitation spectrum) in the range which corresponds to transitions from the ground state to the ${}^4F_{5/2}$ and ${}^4F_{7/2}$ states (full line). The photoacoustic spectrum (PAS) versus wavelength is also shown (dotted line). Both spectra have been normalized.

At this point we should mention the relatively good agreement of this quantum efficiency with that estimated from the analysis of the absorption/emission intensities in terms of the Judd–Ofelt formalism (0.18) [18]. This agreement indicates that this low quantum efficiency can be attributed to non-radiative losses, rather than to other channels such as energy transfer. These losses may be due to a concentration quenching because of the high Nd concentration and/or to a high multiphonon relaxation rate from the metastable state ${}^4F_{3/2}$. A comparison of the fluorescence lifetime ($56 \mu\text{s}$) of our laser crystal with that obtained for low Nd content [17] ($60 \mu\text{s}$) indicates that only a quantum efficiency of about 0.93 should be obtained by the concentration effect. Thus the low quantum efficiency experimentally determined must be mainly due to a high multiphonon relaxation rate from the state ${}^4F_{3/2}$. Moreover, this is in good agreement with the highest energy phonons (1346 cm^{-1}) in YAB [19], so that only about three of these phonons are necessary to fill the energy gap from the state ${}^4F_{3/2}$ to the lower state ${}^4I_{15/2}$.

In summary, a quantum efficiency $\Phi = 0.26$ has been determined for the Nd:YAB self-frequency-doubling laser as a result of a high multiphonon relaxation involving three effective phonons of 1346 cm^{-1} rather than an Nd concentration quenching. This high multiphonon relaxation rate gives rise to the thermal heating effects that strongly influence the laser performance of this material.

Acknowledgments

This paper has been supported by the Comisión Internacional de Ciencia y Tecnología (CICYT) under project MAT 95/152. D Jaque thanks the Ministerio de Educación y Ciencia for a grant.

References

- [1] Fan T Y, Cordova-Plaza A, Dignonnet M J F, Nyer R L and Shaw H J 1986 *Opt. Soc. Am. B* **3** 140
- [2] Lin J T 1990 *Laser Optron.* December, 35
- [3] Lin J T 1990 *Opt. Quantum Electron.* **22** S283
- [4] Capmany J, Bausá L E, Jaque D, García Solé J and Kaminskii A A 1997 *J. Lumin.* **72–74** 816
- [5] Capmany J, Jaque D, García Solé J and Kaminskii A A 1998 *Appl. Phys. Lett.* **72** 531
- [6] Bartschke J, Knappe R, Boller K J and Wallenstein R 1997 *IEEE J. Quantum Electron.* **QE-33** 2295
- [7] Lu Bao-sheng, Wang Ju, Pan Heng-fu, Jiang Min-hua, Liu En-quan and Hou Xue-yuan 1989 *J. Appl. Phys.* **66** 6052
- [8] Tingjie Z, Zundu L, Yichuan H, Min Wang Q and Guang C 1994 *Opt. Commun.* **109** 115
- [9] Hemmati H 1992 *IEEE J. Quantum Electron.* **QE-28** 1169
- [10] Li Zhenhua, Fan Qikang, Zhou Fuzheng, Ma Jianwei and Xue Qiang 1994 *Opt. Eng.* **33** 1138
- [11] Omatsu T, Kato Y, Shimosegawa M, Hasegawa A and Ogura Y 1995 *Opt. Commun.* **118** 302
- [12] Murphy J C and Aamodt M C 1977 *J. Appl. Phys.* **48** 3502
- [13] Merkle L D and Powell R C 1997 *Chem. Phys. Lett.* **46** 303
- [14] Quimby R S and Yen W N 1978 *Opt. Lett.* **3** 181
- [15] Etxebarria J and Fernández J 1983 *J. Phys. C: Solid State Phys.* **16** 3803
- [16] Rodriguez E, Tocho J O and Cussó F 1993 *Phys. Rev. B* **47** 14049
- [17] Luo Zun-Du 1994 *Progr. Natural Sci.* **4** 504
- [18] Jaque D, Capmany J, Luo Z D and García Solé J 1997 *J. Phys.: Condens. Matter* **44** 9715
- [19] Pan Heng-fu, Liu Ming-guo, Xue Jing and Lu Bao-sheng 1990 *J. Phys.: Condens. Matter* **2** 4525